DEVELOPMENT OF A ROBUST ALTITUDE CONTROL SYSTEM FOR A QUADROCOPTER

J. Rhein, B. Messnarz, Department of Aviation, FH JOANNEUM GmbH, Graz, Austria

Abstract

In this report, we present the development of a robust altitude control system for a quadrocopter. The controller has been developed on the basis of a reasonable simple mathematical model. Therefore it must not be sensitive to deviations of the real system from the plant model, which is taken into consideration for controller design. Furthermore, the control system shall be adaptable for different types of input sensor data (e.g. pressure altitude, GPS, or SLAM position measurements). Since the quadrocopter should be able to operate outdoor, a good rejection of external disturbances such as wind gusts should be provided as well. Taking into account all the constraints mentioned above, the control system should still ensure good tracking performance. After the definition of a linear model for the vertical quadrocopter motion, the plant parameters were identified by an iterative comparison of simulation and experiment results. Based on this plant model an altitude control system has been developed according to the Linear Quadratic Gaussian (LQG) design with Loop Transfer Recovery (LTR) in order to fulfill the robustness requirements mentioned above. The LQG design includes a full state feedback controller as well as a Luenberger observer to provide estimates of the system states which cannot be measured.

1. INTRODUCTION

The development of unmanned aerial vehicles (UAV) has become a common field of interest in the aviation industry in the recent years. As in the beginning of UAV development the design was mainly driven by military applications, nowadays more and more possible civil fields of application emerge. These include search and rescue missions, environmental observation tasks, inspection of buildings and electricity pylons and traffic observation. The design of suitable UAV airframes and flight control systems is driven by companies as well research institutions and universities.

One class of UAV that is very popular for flight control system development are so called quadrocopters. An example is shown in figure 1. The configuration with four rotors makes it highly agile and holds out the prospect of a variety of effective control methods. The other advantages of a quadrocopter include:

- Modular set up enables easy modifications with advanced sensors or other equipment
- Small size provides the possibility of indoor experiments
- High payload
- Reasonable low price

There has already been a lot of progress in the development of position control systems for quadrocopters: In [9], [10] and [11] remarkable tracking accuracy and performance has been achieved, even for high speed manoeuvres on strongly curved trajectories. However, this control approaches rely on a visual motion tracking system as it has been described in [1]. Such a system restricts the range of applications for the robot, since it only fulfills the required tasks in a known, defined environment. An alternative approach for position determination and navigation is the so-called *Simultaneous Localization and Tracking* (SLAM) method [5]. It works indoor as well as outdoor and is fully independent of external signal sources such as GPS satellites. A common method to improve the performance of the SLAM algorithm is the fusion of SLAM and inertial measurement unit (IMU) data [2].

In this context this paper deals with the development of an altitude control system for a quadrocopter. The controller has been developed on the basis of a reasonable simple mathematical model. Therefore the control algorithm must not be sensitive to deviations of the real system from the plant model. Furthermore, the control system shall be adaptable for different types of input sensor data (e.g. pressure altitude, GPS, or SLAM position measurements). Since the quadrocopter should be able to operate outdoor, a good rejection of external disturbances such as wind gusts should be provided as well. The complete control algorithm should be executed onboard, therefore the control system must not be too complex since the computation power of the onboard microprocessor is limited. Taking into account all the contraints mentioned above, the control system should still ensure good tracking performance. From these points, the following set of requirements can be stated:

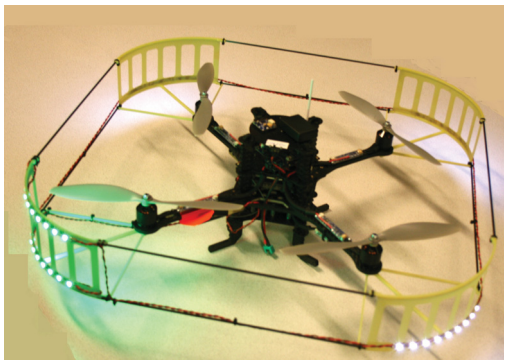

Figure 1: Asctec Pelican quadrocopter used as test bed for the developed controller. The Pelican is equipped with GPS-, IMU- and pressure sensors. It comes with an autopilot board that has a low level processor for data fusion and stabilization and a high level processor for user applications.

- Robustness with respect to plant parameter variations
- Robustness with respect to measurement noise
- Robustness with respect to process noise
- Good reference signal tracking performance
- Vanishing steady-state tracking error
- Simple control system architecture

The chosen design technique is the Linear Quadratic Gaussian (LQG) design with Loop Transfer Recovery (LTR) as it has been described in standard control engineering and flight control systems literature [4], [6], [7], [8], [12], [13]. The LQG design approach includes the design of a full state feedback controller as well as a Luenberger observer to provide estimates of the system states which cannot be measured. A disadvantage is the high number of design parameters, which have to be adapted to ensure that the system meets the requirements. However, with the Loop Transfer Recovery approach, there is an effective method available to decouple the feedback controller design from the observer design and thereby make the entire design process more clear. Besides, the number of design parameters can be reduced to few scalar values, which can be carefully chosen to receive a good tradeoff between robustness and performance. Additionally, the system is augmented by an integrating action in order to improve the tracking performance.

2. PLATFORM DESCRIPTION

The platform used as test bed for controller development is a AscTec Pelican quadrocopter (figure 1). It is equipped with an autopilot board and comes with predefined stabilization and attitude control algorithms. The vehicle's attitude is determined by inertial reference units (IMUs). Lateral Position estimates are available from GPS measurements that are fused with accelerometer readings. A pressure altimeter provides an altitude signal, that is fused with accelerometer data as well.

The autopilot board is equipped with two microprocessors, a Low-Level (LL) and a High-Level (HL) processor. Almost all sensor data is processed and fused on the LL processor. The predefined control algorithms are executed on the LL processor as well. The LL processor code is protected and thereby not available for user applications. However, the fused sensor data is communicated to the HL processor via a serial interface, so that all data is available for control purposes. The HL processor is reserved for user applications. It is freely programmable and can transmit attitude and thrust commands to the LL processor. As an alternative, the attitude controller can be bypassed, so that the motor controllers are directly actuated by the HL processor.

3. CONTROL THEORY FOUNDATIONS

3.1. Linear Quadratic Gaussian Control

Linear Quadratic Gaussian (LQG) control is based on a linear, time-invariant plant model that is disturbed by process and measurement noise:

$$\begin{aligned} \dot{\mathbf{x}} &= \mathbf{A}\mathbf{x} + \mathbf{B}\mathbf{u} + \mathbf{B}_w\mathbf{w}\ ,\ \mathbf{w} \sim (0, \mathbf{Q}_n) \\ \mathbf{y} &= \mathbf{C}\mathbf{x} + \mathbf{D}\mathbf{u} + \mathbf{v}\ ,\ \mathbf{v} \sim (0, \mathbf{R}_n) \end{aligned} \tag{1}$$

where $\mathbf{x}$ is the plant state vector, $\mathbf{u}$ is the input vector and $\mathbf{y}$ is the output vector. The matrices $\mathbf{A}$, $\mathbf{B}$, $\mathbf{C}$ and $\mathbf{D}$ are the state matrix, input matrix, output matrix and feedthrough matrix of the plant. The vector $\mathbf{v}$ is the measurement noise, $\mathbf{w}$ is the process noise, and $\mathbf{B}_w$ is the process noise input matrix. The vectors $\mathbf{v}$ and $\mathbf{w}$ are uncorrelated, unbiased white noise processes, with the covariance matrices $\mathbf{R}_n$ and $\mathbf{Q}_n$.

Figure 2 shows the structure of a LQG controller. Basis for the LQG controller is a Linear Quadratic Regulator (LQR) where all system states are fed back by a feedback gain matrix $\mathbf{K}$. An optimal solution for $\mathbf{K}$ can be found from:

$$\mathbf{K} = -\mathbf{R}^{-1}\mathbf{B}^T\mathbf{X}\ , \tag{2}$$

where $\mathbf{X}$ is the solution of the algebraic

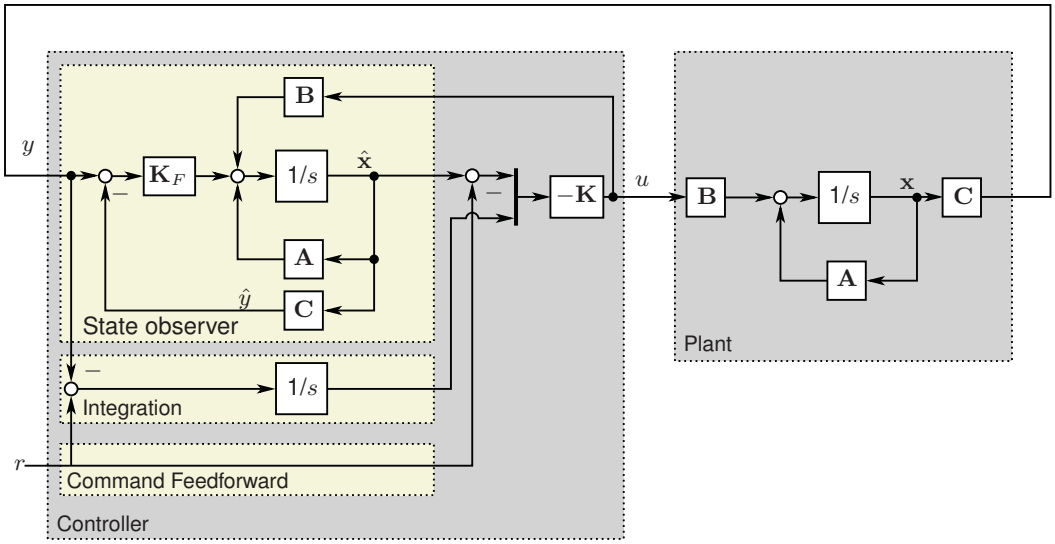

Figure 2: Structure of the LQG controller with integrator augmentation at the plant output. The controller includes a Luenberger observer for state estimation as well as a command feedforward channel and an integrator channel.

Matrix-Riccati-Equation (ARE) [8, p. 126]:

$$0 = \mathbf{A}^T\mathbf{X} - \mathbf{X}\mathbf{A} + \mathbf{X}\mathbf{B}\mathbf{R}^{-1}\mathbf{B}^T\mathbf{X} - \mathbf{Q} \tag{3}$$

The matrices $\mathbf{Q}$ and $\mathbf{R}$ in (2) and (3) are design parameters, that define the behavior of the resulting regulator.

The LQR principle requires knowledge of the complete state vector. However, only the quadrocopter altitude is measured here. Therefore the controller is extended by a Kalman filter, that estimates the unknown system state based on received measurements. This combination of the LQR with a state observer is referred to as Linear Quadratic Gaussian (LQG) control. The observer gain matrix $\mathbf{K}_F$ can be found from:

$$\mathbf{K}_F = \mathbf{X}\mathbf{C}^T\mathbf{R}_n^{-1}\,, \tag{4}$$

where $\mathbf{X}$ is the solution to the ARE:

$$0 = \mathbf{A}\mathbf{X} + \mathbf{X}\mathbf{A}^T - \mathbf{X}\mathbf{C}^T\mathbf{R}_n^{-1}\mathbf{C}\mathbf{X} + \mathbf{B}_w\mathbf{Q}_n\mathbf{B}_w^T \tag{5}$$

3.2. Loop Transfer Recovery

It can be shown, that the linear quadratic regulator has certain guaranteed robustness properties, namely an “infinite” gain margin and a phase margin of at least 60°. Additionally, the LQR remains stable for all model uncertainties, where $m(\omega) < 1/2$ [12, p. 566 f.]. Unfortunately, these properties do not apply automatically for the combination of the LQR with a Luenberger observer that is described in the previous section. This calls for a design of the state observer that recovers the loop transfer properties of the LQR. In order to achieve this goal, the LQG/LTR approach is a method for the proper selection of the design parameters of the LQR as well as the observer. The name arises from the fact that the elements of a Linear Quadratic Gaussian controller (LQG) are determined in a way that promises loop transfer recovery (LTR). First, a state feedback controller is designed according to the equations (2) and (3). The final design should satisfy the robustness requirements and show a good performance. Then a Kalman filter is designed using equation (4) and equation (5). To achieve loop transfer recovery, the following design parameters are chosen:

$$\mathbf{B}_w = \mathbf{I} \tag{6a}$$

$$\mathbf{Q}_n = \mu^2\mathbf{Q}_{n_0} + \mathbf{B}\mathbf{B}^T \tag{6b}$$

$$\mathbf{R}_n = \mu^2\mathbf{R}_{n_0} \tag{6c}$$

where $\mathbf{Q}_{n_0}$ and $\mathbf{R}_{n_0}$ are the initial noise covariance matrices of the plant model. Using this set of parameters it can be shown that for sufficient small values of μ the loop gain of the entire system approaches the loop gain of the LQR [12, p. 570 ff.]. Note that the filter design can be further simplified when choosing $\mathbf{Q}_{n_0}$ and $\mathbf{R}_{n_0}$ as identity matrices. This simplification can be made, since the influence of $\mathbf{Q}_{n_0}$ and $\mathbf{R}_{n_0}$ decreases quadratically with decreasing values of μ.

4. CONTROLLER DEVELOPMENT

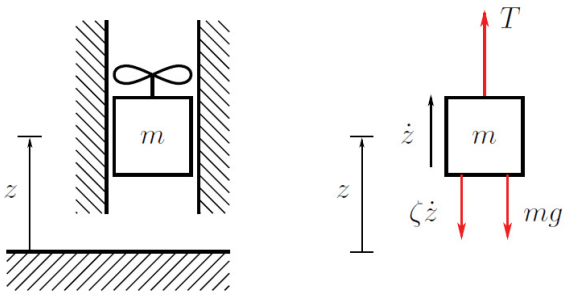

Figure 3: Plant model. The vertical quadrocopter motion is modeled by a point mass under the influence of the gravity and a velocity-dependend damping force. The quadrocopter can be controlled by a thrust force in z-direction, that is the PT_1 response to a thrust command signal.

4.1. Plant Model

Since in this paper only the vertical motion of the quadrocopter is considered, the quadrocopter is modeled as a point mass that is restricted to move only in z-direction as shown in figure 3. Additionally to the thrust force T and the gravity $G = mg$, a velocity-dependent damping force $\zeta\dot{z}$ is introduced. The quadrocopter motion in z-direction is then described by:

$$m\ddot{z} + \zeta\dot{z} = T - mg \tag{7}$$

The actually applied thrust T is modeled as the simple lag filtered response to a dimensionless thrust command T_c that is amplified by a constant factor T_{max}:

$$\dot{T} = \frac{T_c \cdot T_{max} - T}{\tau}\ ,\ T_c \in [0, 1]\ , \tag{8}$$

where τ is the thrust system time constant. However, in order to enable the application of the LQG/LTR design the integrating action of the controller is described as part of the plant model. Therefore an additional state is required:

$$x_I = \int (r - y)\mathrm{d}t \tag{9}$$

The state vector of the plant is then defined as $\mathbf{x} = [z\ \dot{z}\ T\ x_I]^T$.

The plant parameters are identified by an iterative comparison of simulation results and experimental data: In an iteration loop the identification routine minimizes a quadratic cost index that is calculated according to:

$$\begin{aligned} J \quad = \quad & \sum_{i=1}^{n_{Data}} \big[(z_{sim,i} - z_{exp,i})^2 + \\ & \alpha_1(\dot{z}_{sim,i} - \dot{z}_{exp,i})^2 + \\ & \alpha_2(\ddot{z}_{sim,i} - \ddot{z}_{exp,i})^2\big] \end{aligned} \tag{10}$$

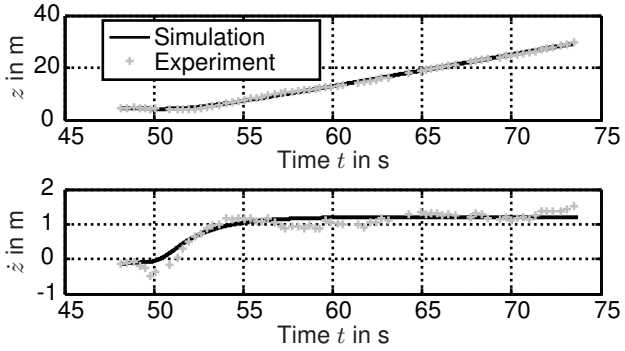

Figure 4: Simulation results after the parameter identification compared to experimental results.

Table 1: Plant parameters

Parameter	Nominal	Min	Max
m	1.7	1.65	2.45
τ	0.0487	0.01	0.1192
ζ	0.4286	0.2395	0.6176
T_{max}	43.5417	41.9049	45.1786

The factors α_1 and α_2 in equation (10) allow for an individual weighting of velocity and acceleration in the cost function.

Figure 4 shows a comparison of the simulation results after the parameter identification and the corresponding experimental data, using the weighting factors $\alpha_1 = 1.0$ and $\alpha_2 = 0.5$. Note that the parameter identification was carried out several times for sequences of climb and descend flights in order to gain data for statistical considerations. The results of the parameter identification are shown in table 1.

4.2. Frequency Domain Robustness Requirements

The basis for the controller development process are robustness requirements that are formulated based on the open loop transfer function of the system in the frequency domain. The examined quantities are:

$$L(s) \quad = \quad G(s)K(s) \quad \text{(Loop gain)} \tag{11}$$

$$D(s) \quad = \quad 1 + L(s) \quad \text{(Return difference)} \tag{12}$$

$$T(s) \quad = \quad D(s)^{-1}L(s) \quad \text{(Cosensitivity)} \tag{13}$$

where $G(s)$ refers to the plant transfer function and $K(s)$ refers to the controller transfer function. Robustness with respect to process and measurement noise can be formulated in terms of $L(s)$: For robustness against process noise, the value of $A(L(s))$ should be high at

low frequencies, while for robustness against measurement noise, the value of $A(L(s))$ should be low at high frequencies. Defining a desired system bandwidth of 10 rad/s, according to [8, p. 154 f.], the following boundaries for the loop gain can be formulated:

(14a) $$A(L(s)) > \frac{10}{\omega} \quad \ldots \omega \leq 1 \text{ rad/s}$$

(14b) $$A(L(s)) < \frac{20}{\omega} \quad \ldots \omega \geq 200 \text{ rad/s}$$

Stability margins are formulated as a minimum value for the return difference:

(15) $$A(D(s)) > -3dB$$

For the derivation of the robustness bounds for plant parameter variations a state-space model that is disturbed by additive uncertainties is considered:

(16) $$\begin{aligned} \dot{\mathbf{x}} &= (\mathbf{A} + \Delta\mathbf{A})\mathbf{x} + (\mathbf{B} + \Delta\mathbf{B})\mathbf{u} \\ \mathbf{y} &= (\mathbf{C} + \Delta\mathbf{C})\mathbf{x} \end{aligned}$$

The uncertain transfer function is then given by [12, p. 534]:

(17) $$G'(s) = G(s) + \Delta G(s) \ ,$$

where

(18) $$\begin{aligned} \Delta G(s) &= \mathbf{C}(s\mathbf{I} - \mathbf{A})^{-1}\Delta\mathbf{B} \\ &\quad + \Delta\mathbf{C}(s\mathbf{I} - \mathbf{A})^{-1}\mathbf{B} \\ &\quad + \mathbf{C}(s\mathbf{I} - \mathbf{A})^{-1}\Delta\mathbf{A}(s\mathbf{I} - \mathbf{A})^{-1}\mathbf{B} \end{aligned}$$

From (18), a lower bound for the cosensitivity can be defined [12, p 526 f.]:

(19) $$A(T(s)) < \frac{1}{m(\omega)} \ ,$$

where $m(\omega)$ is given by:

(20) $$m(\omega) = \left|\Delta G(j\omega) G^{-1}(j\omega)\right|$$

For the determination of $m(\omega)$ the minimum and maximum values of the plant parameters according to table 1 are taken into account. In an iterative routine every possible combination of minimum and maximum values was used to determine the boundary $1/m(\omega)$ according to the equations (18) and (20). This results an array of different curves for $1/m(\omega)$. The final boundary that is shown in figure 7 is determined as the minimum of all curves.

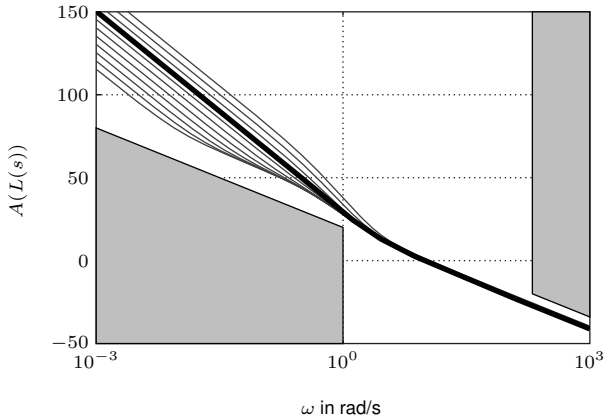

Figure 5: Loop gain plots and robustness boundaries of the regulator for $R = 10^{-2}$ and $\mathbf{Q} = \text{diag}([1\ 0.1\ 0\ q_I])$, where q_I varies in the range $[10^{-2},\ 1]$. The bold line indicates the final choice of $q_I = 0.5$.

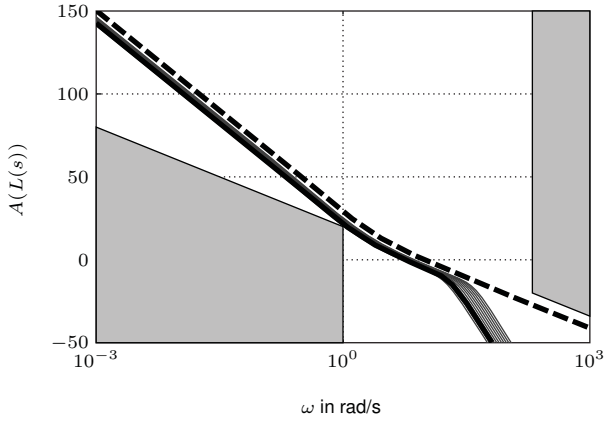

Figure 6: Return difference plots and stability boundaries of the LQG controller for $R_n = 1$ and μ varying in the range $[10^{-4},\ 1]$. The bold line indicates the final choice of $\mu = 0.01$.

4.3. Regulator Design

In a first step the LQR is designed assuming that all system states are perfectly known. The design parameters $\mathbf{Q}$ and $\mathbf{R}$ are varied as follows:

(21a) $$\mathbf{Q} = \text{diag}([1\ 0.1\ 0\ q_I]) \ , \ 10^{-2} \leq q_I \leq 1$$

(21b) $$\mathbf{R} = R \ , \ 10^{-3} \leq R \leq 1$$

An examination of the influence of R has shown that a value of 10^{-2} results in the desired bandwidth of 10 rad/s. Figure 5 shows the resulting loop gain curves for varying values of the integrator weighting factor q_I. A value of $q_I = 0.5$ results in satisfactory robustness against process- and measurement noise.

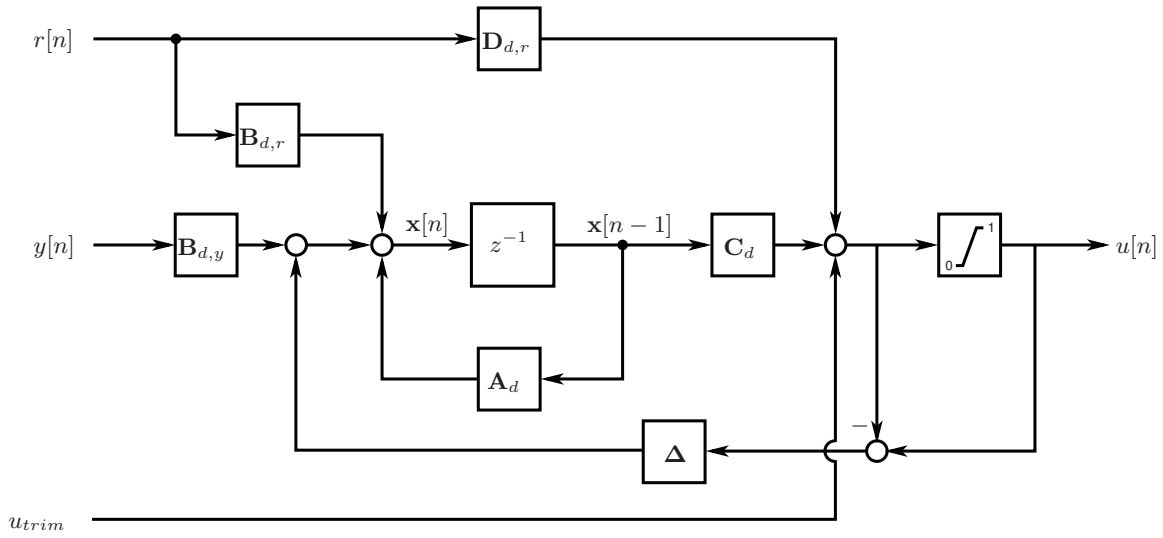

Figure 8: Digital controller layout. As well as the continuous time controller, the digital controller features an integration channel and command feedforward. Additionally, an anti-reset-windup system is included.

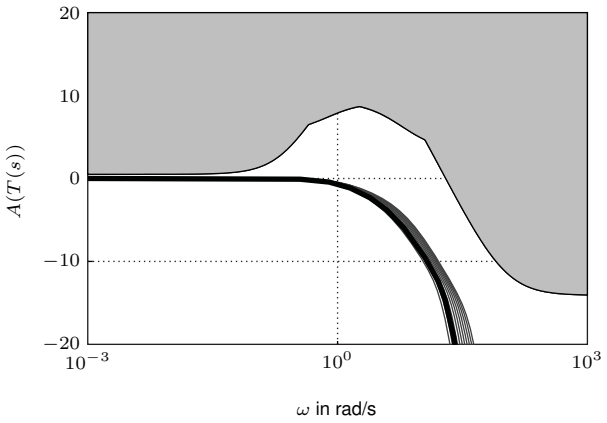

Figure 7: Cosensitivity plots and robustness boundaries of the LQG controller for $R_n = 1$ and μ varying in the range $[10^{-4},\ 1]$. The bold line indicates the final choice of $\mu = 0.01$.

4.4. Observer Design

The Kalman filter is designed according to the equations (5) and (6). Note that for the observer design the plant without integrator augmentation is taken into account. The following design parameters are chosen:

(22a) $\mathbf{Q}_{n_0} = \mathbf{I}$

(22b) $\mathbf{R}_{n_0} = R_n\ ,\ 10^{-4} \leq R_n \leq 1$

(22c) $10^{-4} \leq \mu \leq 1$

Figure 6 shows the loop gain curves for different values of μ, while R_n has been set to 1. The dashed line indicates the loop gain of the LTR without observer that results from the parameters chosen in the previous design step. The loop transfer recovery effect is clearly visible: For decreasing values of μ, the loop gain of the LQG system approaches the loop gain of the LQR without observer. However, too low values of μ result in very high values of the elements of the observer gain matrix $\mathbf{K}_F$, which is not favorable. Therefore, finally a value of $\mu = 0.01$ has been chosen (the bold line in figure 6), since this choice still ensures the required robustness.

Figure 7 shows the cosensitivity plots and robustness boundaries of the LQG controller. It can be seen that the boundaries for robustness against plant parameter variations are satisfied with sufficient margins as well.

4.5. Implementation

In order to implement the developed control system on the HL-processor of the quadrocopter, the structure shown in figure 2 was converted to an equivalent discrete-time system using the zero-order hold method. The resulting control system structure is displayed in figure 8. Since the update rate of the HL-processor is 1 kHz, the resulting discrete-time system can be assumed to be quasi continuous. Note that an estimated trim control signal $u_{trim} = mg/T_{max}$ is added to the control input u. This could indeed be achieved by successive integration of the position error, but this takes some time. Therefore, directly adding u_{trim} improves the performance of the system in the first seconds when the controller is switched on. By the matrix $\Delta = [0\ 0\ 0\ \delta]^T$ an additional anti-reset-windup system is implemented. This improves the controller performance

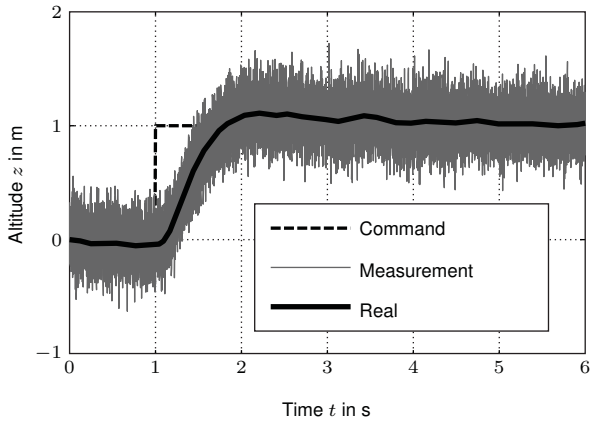

Figure 9: Simulated step response of the controlled system that is perturbed by process and measurement noise. The system responds fast and with a low overshoot.

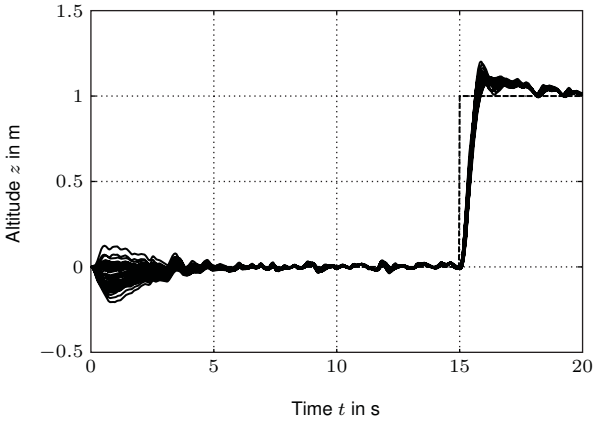

Figure 10: Simulation results of the uncertain plant with randomly varying parameters

when the computed output exceeds the saturation. In this case a signal with complementary sign is added to the integrator in order to prevent a windup.

5. SYSTEM EVALUATION

5.1. Simulation Results

Figure 9 shows the simulated step response of the system that is perturbed by process and measurement noise. The system responds with an overshoot of approximately 5% within a reasonable low time span and no steady-state error remains.

In order to prove the robustness against plant parameter variations the system was simulated repeatedly with parameters that are randomly changed. The result is displayed in figure 10. It can be seen that the system remains stable in all cases. At the beginning of the simulation the self-trimming behavior of the controller that

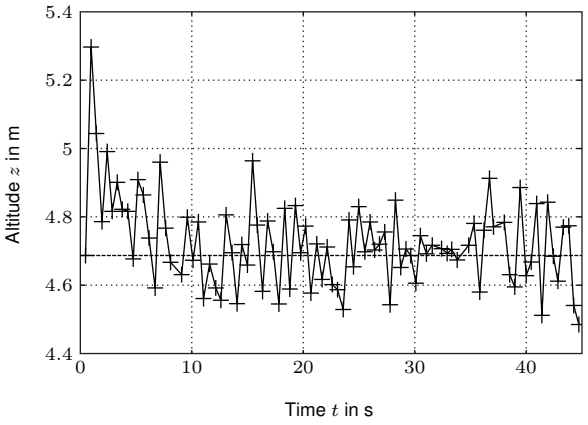

Figure 11: Quadrocopter altitude during controlled hover flight. The dashed line indicates the constant reference altitude. After the hover flight is established, a position accuracy of approximately $\pm$ 20 cm is achieved.

results from the integrator augmentation can be observed. After a maximum time of 6 s the controller establishes steady hover flight that is only disturbed by the influence of process and measurement noise. In the reaction to the 1 m step command a maximum overshoot of 20% is observed. This is still a good result considering that in this simulation the plant dynamics differ significantly from the nominal model.

5.2. Flight Experiments

Figure 11 shows the quadrocopter altitude when a constant altitude command signal is given. The dashed line indicates the constant reference altitude. Just as in the simulations, after a time of about 5 s the hover flight is established. Then a position accuracy of approximately $\pm$ 20 cm is achieved.

Figure 12 shows the quadrocopter response to a 5 m altitude step command. In the beginning of the experiment it can be seen that the real quadrocopter weights less than the nominal mass, since initially to much thrust is applied. The controller compensates for this deviation within a few seconds. For reasons of comparison the results of a simulation, using the same step input signal, are plotted against the experiment results. A remarkable good compliance can be observed. This indicates that the developed controller fulfills the requirement for robustness against plant parameter variations, since it behaves as expected even under real conditions.

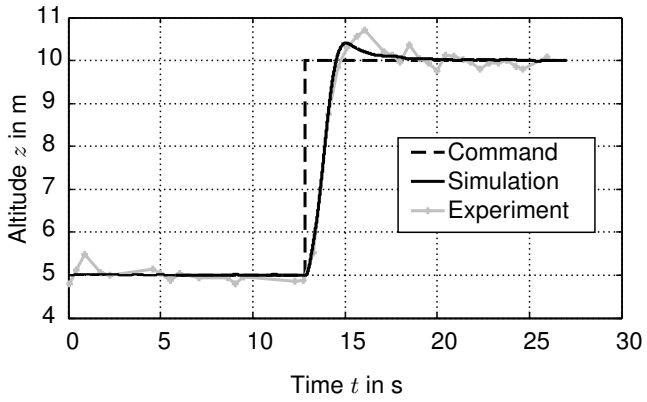

Figure 12: Quadrocopter altitude during a 5 m step command and simulation results for the same input signal.

6. SUMMARY AND OUTLOOK

A robust altitude control system for a quadrocopter was developed based on the LQG/LTR approach. The control system shows good tracking performance and satisfies the required robustness specifications. Based on the design process presented in this paper the existing altitude control system can be extended to a full three-dimensional trajectory controller. Using the attitude control system provided by AscTec this can be done with minimum effort: When the attitude dynamics of the quadrocopter are inverted the high-level trajectory controller can directly command the force components in all three directions as proposed in [3]. Thereby, the principles and design tools used for the development of the altitude controller can directly be applied to the lateral position control.

References

[1] Achtelik, M., Zhang, T., Kiihnlenz, K., and Buss, M., "Visual Tracking and Control of a Quadcopter Using a Stereo Camera System and Inertial Sensors," *Proceedings of the 2009 IEEE, International Conference on Mechatronics and Automation*, Changchun, China, August 2009, pp. 2863–2869.

[2] Achtelik, M., Achtelik, M., Weiss, M., and Siegwart, M., "Onboard IMU and Monocular Vision Based Control for MAVs in Unknown In- and Outdoor Environments," *2011 IEEE International Conference on Robotics and Automation*, Shanghai International Conference Center, Shanghai, China, May 2011, pp. 3058–3063.

[3] Bloesch, M., Weiss, S., Scaramuzza, D., and Siegwart, R., "Vision Based MAV Navigation in Unknown and Unstructured Environments," *2010 IEEE International Conference on Robotics and Automation (ICRA)*, 2010, pp. 21–28.

[4] Brockhaus, R., *Flugregelung*, 3rd ed., Springer-Verlag, Berlin, 2000.

[5] Dissanayake, M., Newman, P., Clark, S., Durrant-Whyte, H., and Csorba, M., "A solution to the simultaneous localization and map building (SLAM) problem," *IEEE Transactions on Robotics and Automation*, 3, Vol. 17, June 2001, pp. 229 – 241.

[6] Ducard, G., *Fault-tolerant Flight Control and Guidance Systems*, Springer-Verlag, London, Great Britain, 2009.

[7] Föllinger, O., *Regelungstechnik*, 10th ed., Huethig Verlag, Heidelberg, Germany, 2008.

[8] Geering, H. P., *Regelungstechnik*, 5th ed., Springer-Verlag, Germany, 2001.

[9] Lupashin, S., Schöllig, A., and Sherback, M., "A Simple Learning Strategy for High-Speed Quadrocopter Multi-Flips," *IEEE International Conference on Robotics and Automation*, 2010, pp. 1642–1648.

[10] Mellinger, D. and Kumar, V., "Minimum Snap Trajectory Generation and Control for Quadrotors," *IEEE International Conference on Robotics and Automation*, Shanghai International Conference Center, May 2011, pp. 2520–2525.

[11] Schoellig et al., "Synchronizing the Motion of a Quadrocopter to Music," *2010 IEEE International Conference on Robotics and Automation*, Anchorage Convention District, Anchorage, Alaska, USA, May 2010, pp. 3355–3360.

[12] Stevens, B. and Lewis, F., *Aircraft Control and Simulation*, 2nd ed., John Wiley & Sons, Inc., Hoboken, New Jersey, 2003.

[13] Tewari, A., *Modern Control Design*, John Wiley & Sons, Inc., Baffins Lane, Chichester, West Sussex, PO19 1UD, England, 2002.